Elemental and morphological analyses of filter tape deposits from a beta attenuation monitor

John G. Watson [a,b,*], Judith C. Chow [a,b], L.-W. Antony Chen [a], Steven D. Kohl [a], Gary S. Casuccio [c], Traci L. Lersch [c], Rodney Langston [d]

[a] Division of Atmospheric Sciences, Desert Research Institute, 2215 Raggio Parkway, Reno, Nevada 89512, USA
[b] State Key Laboratory of Loess and Quaternary Geology, Institute of Earth Environment, Chinese Academy of Science, 10 Fenghui South Road, Xi'an High-Tech Zone, Xi'an, 710075, China
[c] RJ Lee Group, Inc., Monroeville, Pennsylvania, USA
[d] Department of Air Quality and Environmental Management, Clark County, Las Vegas, Nevada, USA

ARTICLE INFO

ABSTRACT

An hourly average PM_{10} concentration of 1402 $\mu g\ m^{-3}$ was registered at 1400 Pacific Standard Time (PST), 1/11/2007, on the beta attenuation monitor (BAM) at a North Las Vegas, Nevada sampling site. The high PM_{10} concentration at ~1245–~1331 PST was a microscale event, limited strictly to the PM_{10} sampler; it did not affect the adjacent $PM_{2.5}$ concentrations. A method was developed for retrospective compositional analysis of BAM glass-fiber filter tape sample deposits. Sample punches were submitted for optical examination, followed by elemental and morphological analyses with X-ray fluorescence (XRF) and scanning electron microscopy (SEM)-energy dispersive X-ray spectroscopy (EDS) analyses, respectively. Geological samples surrounding the sampling site were acquired to establish source profiles and identify source markers.

Although blank levels for many elements were high on the glass-fiber filter tape from the BAM, they were consistent enough to allow background subtraction from the deposit concentrations for most chemical components. Chemical mass balance (CMB) receptor model source apportionment for the event closely matched the paved road dust sample collected adjacent to the sampling site. It is likely that this high mass event was the result of environmental vandalism. This study demonstrates the feasibility of analyzing BAM filter tape deposits for source attribution, especially for short-duration fugitive dust events. Filter tapes should be time-stamped and immediately retained after an event for future analysis.

© 2011 Elsevier B.V. All rights reserved.

1. Introduction

Beta attenuation monitors (BAMs) (Lillienfeld, 1970) measure $PM_{2.5}$ and PM_{10} (particles with aerodynamic diameters less than 2.5 and 10 micrometers [μm], respectively) concentrations by drawing ambient air through a filter tape and quantifying the decreasing transmission of electrons (β particles) generated by a radioactive source (usually ^{14}C) as the aerosol deposit increases. This exponential attenuation is related to mass through factory calibration against known standards. There is a weak dependence of transmission efficiency on the deposit composition (Jaklevic et al., 1981). The tape advances after the attenuation reaches a pre-set level or at pre-set time intervals (e.g., 1 to 24 hours). When equipped with the appropriate size-selective inlet (Watson and Chow, 2011), BAM PM_{10} and $PM_{2.5}$ measurements are comparable to manual 24-hr filter measurements (Chang et al., 2001; Chang and Tsai, 2003; Chow et al., 2006; Chung et al., 2001; Gehrig et al., 2005; Hauck et al., 2004; Huang

* Corresponding author at: Division of Atmospheric Sciences, Desert Research Institute, 2215 Raggio Parkway, Reno, Nevada, USA. Tel.: +1 775 674 7046; fax: +1 775 674 7009.
E-mail address: john.watson@dri.edu (J.G. Watson).

and Tai, 2008; Kashuba and Scheff, 2008; Takahashi et al., 2008; Tsai and Cheng, 1996; Zhu et al., 2007).

BAMs are usually used for hourly $PM_{2.5}$ or PM_{10} mass concentration measurements, and a few past studies have reported the feasibility of follow-up chemical/physical characterization from BAM tapes. Nakamura and Ise (1999) dislodged suspended particles from the glass-fiber tape, then transferred and redeposited particles onto a polycarbonate filter using a polyvinyl acetate emulsion adhesive. Particle-induced X-ray emission (PIXE) analysis was applied to obtain relative concentrations for sulfur (S), chlorine (Cl), iron (Fe), and zinc (Zn). Saitoh et al. (2006) replaced the BAM glass-fiber tape with Polytetrafluoroethylene (PTFE) ultra-membrane tapes for quantitative analysis of multi-elements by PIXE. Wang et al. (1998) reported a two-step acid digestion of glass-fiber BAM filter tape followed by inductively coupled plasma (ICP)-atomic emission spectrometry (AES) or -mass spectrometry (MS) analyses for 18 elements to investigate Asian dust transport from China to Taiwan. Elevated calcium (Ca), Fe, and magnesium (Mg) concentrations marked the dust events. Using a combination of X-ray diffraction (XRD) and scanning electron microscopy (SEM), Rodriguez et al. (2009) illustrated XRD patterns of $PM_{2.5}$ and PM_{10} samples for northern Spain and identified local and transported pollution sources.

This study demonstrates a method to retrieve deposits and unexposed blank filter aliquots from the BAM glass-fiber tape to quantify elemental concentrations and determine particle morphology. It answers the question: "To what extent can the routinely-acquired BAM tape be further analyzed to explain excessive mass concentrations?" The additional information helps identify PM sources and define the causes of elevated PM concentrations.

The example is a short-duration event detected during the early afternoon of 1/11/2007 at a North Las Vegas, Nevada, sampling site (36°14'43" N; 115°05'36" W) when hourly PM_{10} concentrations reached 1402 µg m^{-3} at 1400 Pacific Standard Time (PST) with a 24-hour average of 155 µg m^{-3}. This site (the Bemis site in Chow et al. (1999), later renamed "Craig Rd.") was affected by fugitive dust in the past, but the U.S. National Ambient Air Quality Standards (NAAQS) for PM_{10} have not been exceeded since 2001. Hypotheses concerning the cause of this excursion were: 1) an instrument malfunction; 2) an unusual meteorological event, such as wind erosion; 3) contributions from one or more nearby industrial activities that might be subject to additional controls; or 4) an unusual short-duration event, such as someone tossing a handful of dirt at the sampling inlet. These hypotheses were investigated by developing a method to analyze portions of the filter tape by X-ray fluorescence (XRF; Watson et al., 1999) for elemental concentrations and SEM (Casuccio et al., 1983) for comparison with the composition of potential fugitive dust sources. The strengths and limitations of the method are evaluated.

2. Methodology

2.1. Ambient Sampling

Hourly $PM_{2.5}$ and PM_{10} concentrations were reported by two BAMs (Model FH62 C-15 Series, Thermo Fisher Scientific, Franklin, Massachusetts, USA) at the North Las Vegas

sampling site shown in Fig. 1. Inlets were situated ~4 m above ground level and the $PM_{2.5}$ inlet was within 2 m of the PM_{10} inlet. This site was located in a light commercial district interspersed with a cinderblock manufacturing facility (for the construction industry) and a concrete ready-mix facility (for an aggregate handling operation) to the northeast; office buildings and an unpaved storage yard to the east; housing developments to the southeast (~1 km); and Interstate highway 15 (I-15) to the west and northeast (~200 m).

The glass-fiber filter tape (#460130; MetOne, Grants Pass, Oregon, USA) used in the BAM is composed of aluminosilicates and contains other elements and compounds that might interfere with chemical analysis. Under normal operating conditions, particle deposits from a sample flow rate of 16.7 L min^{-1} are focused on a 16 mm diameter spot with deposits of less than 1000 µg (average daily PM concentration of 41.67 µg m^{-3}). The tape advances when the BAM detects a pressure drop due to excessive particle loading. The BAM records the time when the tape advances but it does not date-stamp the tape. It was necessary to count spots from the end of the tape to find the region of the occurrence. Fortunately, the tape was changed soon after the event. It would be useful to put a time and date mark on BAM tapes if this methodology is applied in the future.

The filter tape was unrolled in a laminar flow hood and deposit spots were removed with a 25 mm diameter steel punch (C.S. Osborne and Co., Harrison, New Jersey, USA) that was cleaned with methanol (CH_3OH)-soaked Kimwipes (Kimberly Clark, Dallas, Texas, USA) between punches. Each punch was assigned an ID code and stored in an individual PetriSlide (Millipore, Billerica, MA, USA). The unexposed distance between BAM deposit spots is 31.75 mm (1.25"), which allows a 25 mm punch to be taken from the area to determine blank values for subtraction (see Supplemental Figure S-1). For comparison, seven additional sample spots were taken at 2400 PST on 1/11/2007, as well as before (1/06/2007, 1/09/2007 and 1/10/2007) and after (1/12/2007, 1/13/2007 and 1/16/2007) the day of the event. Ambient concentrations (µg m^{-3}) for each sampling spot were calculated by subtracting blank levels and dividing by the product of sample duration and flow rate.

2.2. Laboratory Analyses

Filter punches (i.e., five samples during the event and transition periods, and seven samples before and after the event) were examined under an optical microscope (Leitz Ortholux binocular microscope, Munich, Germany). Notes were taken on the color, homogeneity, and visibility of super-coarse (>10 µm) particles associated with each deposit. No super-coarse particles were observed on the BAM filter tape.

The filter punches were submitted to energy dispersive XRF (ED-XRF) analysis for 51 elements using a PANalytical unit (Model Epsilon 5; Almelo, The Netherlands) following the analytical protocol specified in Supplemental Table S-1. XRF is a non-destructive method, allowing the filter punch to be submitted to other analyses that would destroy the filter (Wang et al., 1998). A multi-element thin-film standard was analyzed with each run to monitor calibration drift. The minimum detection limits (MDLs) were determined using the
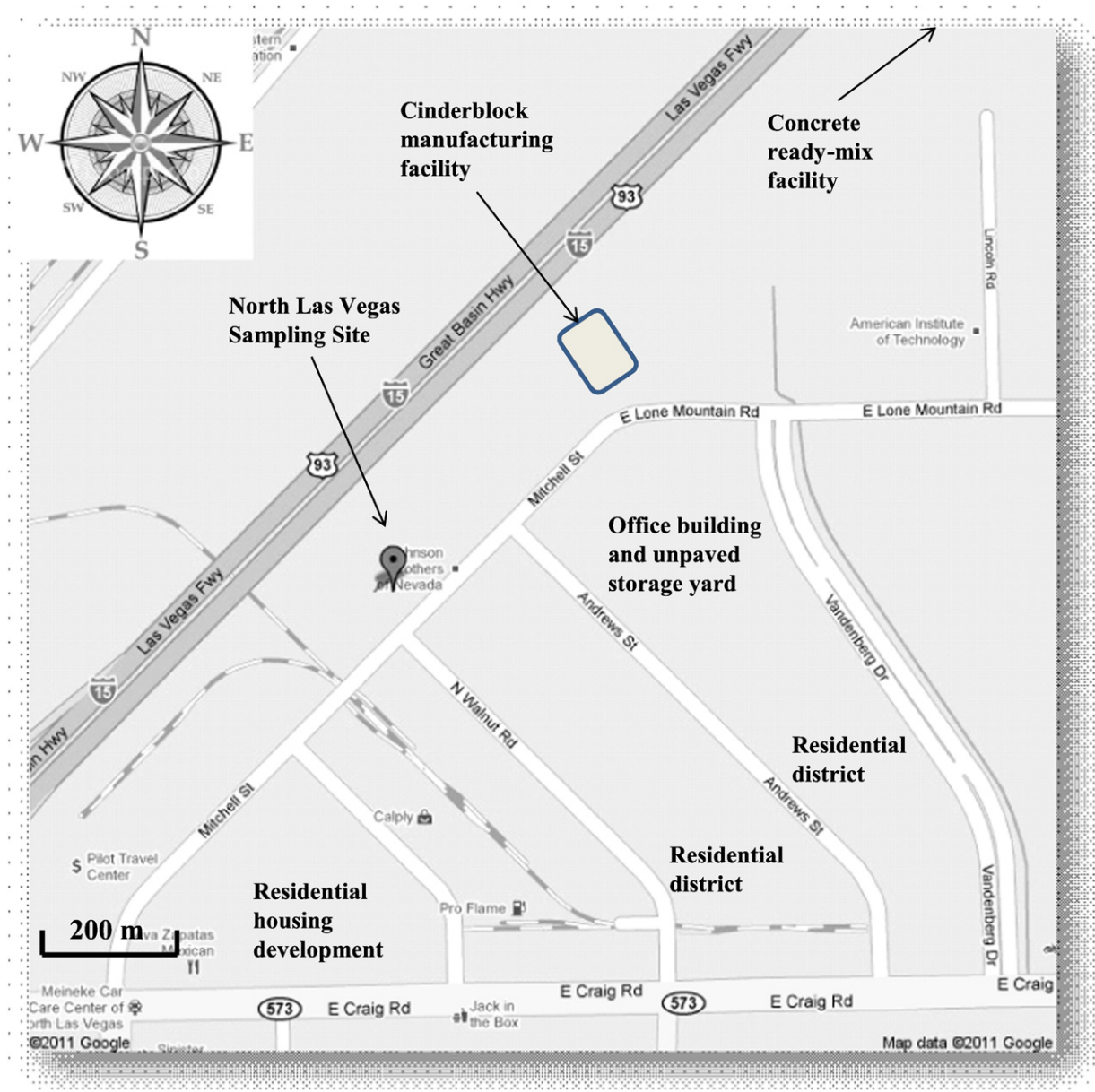
Fig. 1. Surroundings of the North Las Vegas (Craig Road), Nevada sampling site (36°14'43" N; 115°05'36" W).

standard deviation of the concentration measured on the nine unexposed (i.e., non-deposit) punches, which were treated as laboratory blanks (U.S.EPA, 1999). Most of the light elements (i.e., sodium (Na), aluminum (Al), silicon (Si), and phosphorous (P)) were not quantifiable on the BAM deposits due to the high and variable levels (50–280 μg/filter punch) in the unexposed filter tape. Filter blank Mg levels were low (7.1 ± 0.23 μg/filter punch), allowing semi-quantification of Mg concentrations. Blank levels for potassium (K), Zn, and barium (Ba) were also high and variable (57–268 μg/filter punch) and unquantifiable. Most of the other elements showed consistent blank concentration levels with low MDLs.

For SEM-electron dispersive spectroscopy (SEM-EDS) analyses, samples were mounted on a stub with conductive carbon tape, then coated with a thin layer of carbon by evaporative deposition under vacuum. The carbon layer is not detected by the SEM-EDS and is used to dissipate the electron charge induced on the sample by the electron beam. A PERSONAL SEM (RJ Lee Group, Inc., Monroeville, PA) instrument, equipped with a Noran light element EDS detector, was used to characterize particles associated with each ambient sample. The samples were examined manually in the SEM at magnifications ranging from 25x–10,000x using the secondary, backscattered, and EDS detectors. Initially, X-ray spectra for random areas of the filter were collected, providing information on elemental composition similar to bulk XRF analyses. Individual particles were then analyzed using EDS and classified into major and minor groups based on elemental

components and abundances. Digital images and spectra from representative areas of the sample deposit were collected to document key particle types and particle distribution.

2.3. Source Profiles

Geological samples were acquired on 4/18/2007 for bare soil, paved road dust, material from the nearby storage pile of the cinderblock manufacturing facility, and sand from the concrete ready-mix facility as documented in Supplementary Table S-3. These samples were air dried and sieved to 38 μm prior to sample re-suspension onto Teflon-membrane filters (R2PJ047, Pall Life Sciences, Ann Arbor, Michigan, USA) using a PM_{10} size-selective inlet (Chow et al., 1994). These fugitive dust samples were submitted to the same XRF analysis and were used to evaluate the similarities and differences in terms of elemental abundances.

3. Results

$PM_{2.5}$ and PM_{10} concentrations for the period including the event are shown in Fig. 2. Excluding 1/11/2007 as an outlier, PM_{10} mass concentration varied from 6.2 to 53.8 μg m^{-3} during January, with a monthly average of 28.2 ± 13.5 μg m^{-3}. Corresponding $PM_{2.5}$ ranged from 2.4 to 14.5 μg m^{-3}, with a monthly average of 6.8 ± 2.9 μg m^{-3}. $PM_{2.5}$ levels built up over the period from 1/01–04/2007, followed by low concentrations during the period from 1/05–07/2007. A decreasing trend is apparent for both $PM_{2.5}$ and PM_{10} prior to the event (from 1/08–10/2007). Excluding the 1/11/2007 data (PM_{10} and $PM_{2.5}$ of 154.8 and 7.0 μg m^{-3}, respectively), the daily $PM_{2.5}$ to PM_{10} ratio for this site varied around 0.2–0.3, with a monthly average of 0.27 (January 2007), close to the ratio of 0.32 found in January 2006. The low $PM_{2.5}/PM_{10}$ ratio for 1/11/2007 (0.045) is consistent with this being an isolated event dominated by the coarse particle fraction, as evidenced by the diurnal PM_{10} variations shown in Fig. 3a. Hourly PM_{10} increased from 272 μg m^{-3} at 1300 PST to 1402 μg m^{-3} at 1400 PST, and decreased to 905 μg m^{-3} at 1500 PST, with no corresponding increase in $PM_{2.5}$ (which
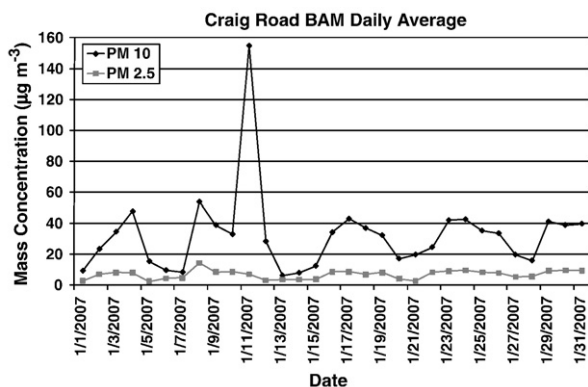

Fig. 2. Daily 24-hour average BAM $PM_{2.5}$ and PM_{10} mass concentrations from the North Las Vegas sampling site for January 2007 (hourly BAM data were averaged to obtain daily concentration; mass concentration data for the month of January 2007 were downloaded from the Clark County website: www.ccairquality.org/archives/index.html).
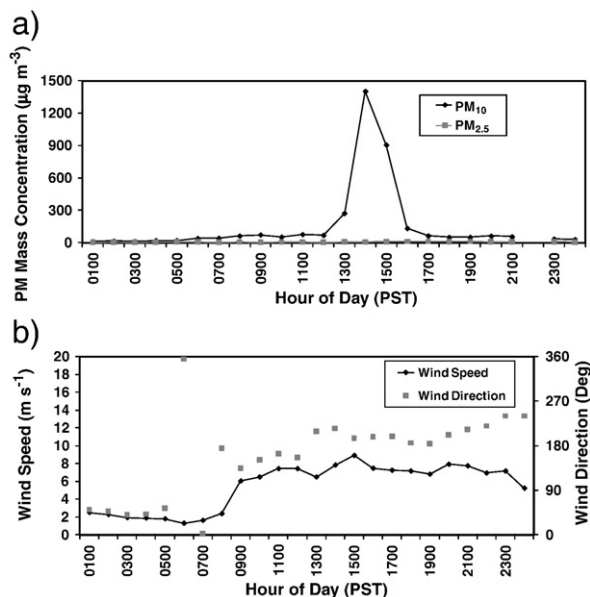

Fig. 3. Diurnal variations in: a) hourly $PM_{2.5}$ and PM_{10} mass concentrations (illustrating the PM_{10} event during the early afternoon), and b) hourly wind speed and wind direction measurements acquired on 1/11/2007 from the North Las Vegas sampling site.

varied in the range of 7–12 μg m^{-3}). The event began at ~1245 PST on 1/11/2007; carryover was cleared by 1700 PST ($PM_{10} = 64$ μg m^{-3}) as the system tape advanced. Fig. 3b shows that wind speeds were moderate (~6–7 m s^{-1}) during the event with southerly and southeasterly flow across the site.

Optical microscopy revealed that the spots taken during the event were lighter in appearance with inhomogeneous deposits (see Figure S-1). Deposit spots taken before and after the event were optically darker with homogeneous deposits (without apparent metallic particles), likely due to the longer (24 hr) sampling times. To assess how deeply particles penetrated the filter and also the effect of rubbed-off material on the filter backing, the back (non-deposit) sides of the filters were analyzed. With the exception of Cl, all of the quantifiable light elements (e.g., Mg, S, and Ca) measured on the non-deposit side were less than 10% of the amount on the deposit side. This indicates that penetration was not deep, consistent with cross-sections examined by Chow et al. (2004) for elemental carbon. Elevated Cl levels can result from filter handling in the field or from collection of a liquid sample (e.g., from the dust-suppression water spray used at the neighboring brick-making facility) that wicks through the filter.

Elements measured above MDLs are compared to the Fe concentration in Table 1 to distinguish differences in elemental ratios before, during, and after the event. Average PM_{10} Fe concentrations varied over two orders of magnitude before (0.85 μg m^{-3}), during (77.17 μg m^{-3}), and after (0.20 μg m^{-3}) the event. Ca/Fe and manganese (Mn)/Fe ratios increased by 33–42% (significant at 5% level) and 63–93%, respectively. Other components also showed increased concentrations during the event.

Table 1
Average elemental to iron (Fe) ratios of BAM tape before, during, and after the 1/11/2007 event [a].

Element	Average Before Event[b]		Average During Event[b]		Average After Event[b]	
	Element to Fe Ratio	Stdev[c]	Element to Fe Ratio	Stdev[c]	Element to Fe Ratio	Stdev[c]
Magnesium (Mg)	0.3099	0.0501	0.4465	0.0207	0.4056	0.1025
Sulfur (S)	0.2686	0.0610	0.2433	0.0105	0.4370	0.1303
Chlorine (Cl)	0.1845	0.1602	0.0590	0.0035	0.8213	0.4977
Calcium (Ca)	5.1357	0.7512	7.3182	0.0798	5.5134	1.2374
Titanium (Ti)	Not Detected	0.0000	0.0163	0.0011	Not Detected	0.0000
Chromium (Cr)	0.1929	0.1662	0.0249	0.0014	0.0346	0.0277
Manganese (Mn)	0.0668	0.0358	0.1092	0.0008	0.0567	0.0652
Iron (Fe)	1.0000	0.0000	1.0000	0.0000	1.0000	0.0000
Nickel (Ni)	0.0172	0.0167	0.0023	0.0005	0.0047	0.0000
Copper (Cu)	0.0195	0.0073	0.0184	0.0017	0.0236	0.0069
Arsenic (As)	Not Detected	0.0000	0.0006	0.0002	Not Detected	0.0000
Bromine (Br)	0.0019	0.0010	0.0005	0.0004	0.0028	0.0000
Rubidium (Rb)	0.0020	0.0008	0.0033	0.0008	0.0035	0.0000
Strontium (Sr)	0.0613	0.0333	0.0636	0.0037	0.0814	0.0328
Yttrium (Y)	0.0022	0.0019	0.0015	0.0004	0.0007	0.0000
Zirconium (Zr)	0.0110	0.0051	0.0095	0.0007	0.0114	0.0039
Molybdenum (Mo)	0.0025	0.0005	0.0017	0.0004	0.0026	0.0003
Silver (Ag)	0.0052	0.0000	0.0009	#DIV/0!	0.0075	0.0000
Cadmium (Cd)	Not Detected	0.0000	0.0028	0.0009	Not Detected	0.0000
Indium (In)	Not Detected	0.0000	Not Detected	0.0000	Not Detected	0.0000
Tin (Sn)	Not Detected	0.0000	0.0010	0.0004	0.0050	0.0042
Antimony (Sb)	0.0034	0.0000	0.0014	0.0000	0.0080	0.0040
Lead (Pb)	0.0062	0.0004	0.0040	0.0021	0.0029	0.0000

[a] Includes only elements detected during one of the three periods.
[b] Before event: 24 hour samples from 1/06/2007, 1/09/2007, and 1/10/2007; during event: 3 samples starting at 1245 PST and ending at 1331PST on 1/11/2007 as shown in Supplemental Table S-2 (Note that transition periods [i.e., immediately before the event and after event clean out: 0000–1245 PST, 1331–1653 PST, and 1653–2400 PST on 1/11/2007] are not included in the calculations); after event: 24 hour samples from 1/12/2007, 1/13/2007, and 1/16/2007.
[c] A standard deviation (Stdev) equal to zero is reported when only one observable was seen for that particular species.

As shown in Supplemental Table S-2, the highest elemental concentrations were reported for the 1245–1257 PST period on 1/11/2007. PM_{10} Ca and Fe concentrations were 687 ± 115 and $93 \pm 5 \, \mu g \, m^{-3}$, 160- to 110-fold higher than those of 1/10/2007, respectively. PM_{10} S concentration also increased by 110-fold from 1/10/2007 $(0.21 \pm 0.01 \, \mu g \, m^{-3})$ to 1245–1257 PST on 1/11/2007 $(23 \pm 1.2 \, \mu g \, m^{-3})$. S in the form of gypsum $(CaSO_4)$ may have caused an increase in S concentration during the event. Ca concentrations also increased for the periods starting 1257 PST $(479 \pm 81 \, \mu g \, m^{-3})$ and 1315 PST $(570 \pm 96 \, \mu g \, m^{-3})$ on 1/11/2007. Table S-2 shows that the sum of species to daily average mass ratio increased by 17-fold, ranging from 0.19 on 1/10/2007 to 5.7 at 1245 PST on 1/11/2007. This is consistent with the short-term rise in mass concentration and demonstrates that the BAM was functioning properly throughout the event.

The PM_{10} mass concentrations in Fig. 3a were higher from ~1300 to ~1500 PST. However, the elemental concentrations (particularly Ca, the dominant species in these samples) indicate a shorter event, starting at 1245 PST and ending by 1331 PST. For the transition period (i.e., after event clean out) PM_{10} Ca concentrations decreased from $99 \pm 17 \, \mu g \, m^{-3}$ (1331–1653 PST) to $71 \pm 12 \, \mu g \, m^{-3}$ (1653–2400 PST). The sum of elements in Supplemental Table S-2 also shows that the event lasted approximately half an hour.

The sample from the cinderblock facility storage pile was resuspended seven separate times to determine the variability of its profile. The standard deviations were less than 1% for each element quantified, with the exception of the most abundant element measured, Si (45%), for which the precisions was $\pm 1.8\%$ (Watson et al., 2007). Among the seven geological samples, Table 2 shows that Ca/Fe ratios varied by threefold, ranging from 7.2 for the cinderblock facility storage pile to 24.7 for the concrete facility sand, equal to or higher than the 7.3 Ca/Fe ratio found on the BAM deposit during the event (shown in Table 1).

Elemental abundances of PM_{10} in Fig. 4 show that the soil and paved road dust samples are similar, with 19.8% and 18.8% Ca, and 9.9% and 12.7% Si, respectively. The cinderblock pile profile contains the lowest Ca (3.7%) and highest Si (44.9%) abundances among the four profiles, suggesting the mixture from the storage pile contains more sand than dolomite, despite the commercial designation of this material as "Dolomite." The Al abundance (16.2%) in the cinderblock pile profile is three times higher than that of soil (4.3%) or paved road dust (5.6%). The level of S (2.3%) in the cinderblock pile sample is also 7–17 times higher than that in soil (0.13%) and paved road dust (0.36%), which may be due to the presence of $CaSO_4$ from the cinderblock manufacturing facility. Individual PM_{10} source profile abundances for the seven geological samples are presented in Supplemental Table S-4.

SEM-EDS analysis was performed for samples on 1/11/2007 as well as 24-hour samples collected before (1/09/2007) and after (1/13/2007) the event as specified in Supplemental Table S-2. Each sample consisted primarily of Ca and Ca/Si-rich particles, usually in a mixture with Al and Mg, as well as Fe and Si/Al-rich particles and a mixture of Na, S, K, Ca, and Fe, either singly or in combination. The remainder of each sample was composed primarily of Si/Oxygen (quartz), Ca/Mg (dolomite), Ca/S (gypsum in both fibrous and non-fibrous forms), Fe/S (pyrite), and Ba/S. Carbon

Table 2
Ratios of source sample elements to iron (Fe) for the seven geological samples acquired in Las Vegas, Nevada.

Sample Type (Sample ID)	Construction Soil (RS800)	Paved Road Dust (RS801)	Soil (RS802)	Mixture of Soil and Paved Road Dust (RS803)	Trackout Dust (RS804)	Material (RS806)	Sand (RS805)
Sampling Location	Craig and Walnut Road[a]	Mitchell Road[b]	Vacant Lot[c]	North Sampling Site Entrance[d]	Cinderblock Facility Entrance Road[e]	Cinderblock Facility Storage Pile[f]	Concrete Facility Sand[g]
Magnesium (Mg)	3.9099	1.8338	3.7507	1.7914	2.5771	2.5509	5.2831
Sulfur (S)	0.1295	0.2088	0.7566	0.0189	0.2113	3.9593	0.2056
Chlorine (Cl)	0.0622	0.0623	0.1466	0.0403	0.0570	0.0352	0.0679
Calcium (Ca)	19.7273	10.8190	20.3966	13.2673	14.2610	7.2101	24.6822
Titanium (Ti)	0.0993	0.0805	0.0912	0.0807	0.1000	0.2516	0.0955
Chromium (Cr)	0.0012	0.0026	0.0013	0.0025	0.0022	0.0065	0.0014
Manganese (Mn)	0.0229	0.0383	0.0243	0.0312	0.0429	0.0240	0.0255
Iron (Fe)	1.0000	1.0000	1.0000	1.0000	1.0000	1.0000	1.0000
Nickel (Ni)	0.0008	0.0002	0.0008	0.0006	0.0007	0.0022	0.0020
Copper (Cu)	0.0012	0.0077	0.0009	0.0045	0.0039	0.0026	0.0028
Arsenic (As)	0.0000	0.0000	0.0000	0.0000	0.0000	0.0000	0.0000
Bromine (Br)	0.0000	0.0000	0.0000	0.0005	0.0001	0.0033	0.0000
Rubidium (Rb)	0.0043	0.0026	0.0037	0.0029	0.0030	0.0057	0.0011
Strontium (Sr)	0.1726	0.0600	0.1298	0.0483	0.0330	0.0501	0.0134
Yttrium (Y)	0.0013	0.0009	0.0005	0.0007	0.0000	0.0015	0.0006
Zirconium (Zr)	0.0075	0.0057	0.0065	0.0034	0.0082	0.0177	0.0105
Molybdenum (Mo)	0.0000	0.0011	0.0005	0.0020	0.0024	0.0024	0.0015
Silver (Ag)	0.0000	0.0011	0.0000	0.0002	0.0000	0.0039	0.0000
Cadmium (Cd)	0.0015	0.0002	0.0004	0.0000	0.0000	0.0011	0.0000
Indium (In)	0.0000	0.0000	0.0000	0.0000	0.0000	0.0000	0.0021
Tin (Sn)	0.0000	0.0000	0.0000	0.0000	0.0000	0.0000	0.0000
Antimony (Sb)	0.0000	0.0000	0.0000	0.0000	0.0000	0.0000	0.0000
Lead (Pb)	0.0000	0.0000	0.0000	0.0000	0.0001	0.0181	0.0000

[a] Consists of soil collected from the southeast corner of Craig and Walnut Road construction.
[b] Road dust collected from the curb at the Mitchell Road entry to sampling site.
[c] A mixture of desert soil, sand, and gravel collected at the southeast corner of the sampling site in a vacant lot.
[d] Mixture of soil and paved road dust collected at the north side of the sampling site entrance.
[e] Trackout dust collected from the entrance road to the cinderblock manufacturing facility.
[f] Material collected from the storage pile of the cinderblock manufacturing facility.
[g] Sand collected from a concrete ready-mix facility.

particles, carbon-chain agglomerates, and salt (NaCl) were also detected. The metallic particle type found in trace amounts consists mostly of spherical and non-spherical chromium (Cr) particles. Fe-rich, titanium (Ti)/Fe, and copper (Cu)-rich particles were also observed. Fig. 5 presents back-
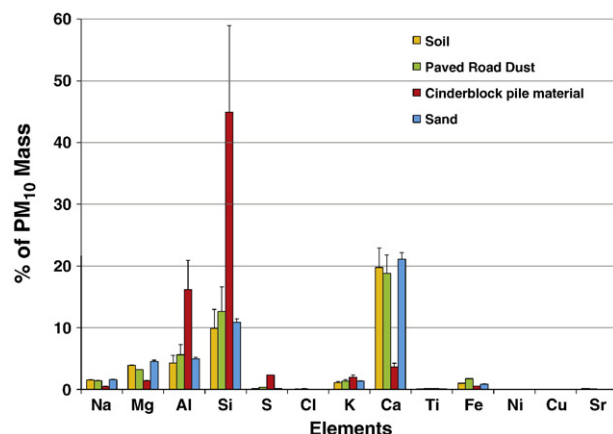

Fig. 4. Comparison of PM$_{10}$ source profiles among construction soil, paved road dust, cinderblock facility storage pile material, and concrete facility sand (Samples RS800, RS801, RS806, and RS805, respectively, in Table 2) collected near the North Las Vegas sampling site. The error bars represent the standard deviation of the individual source sample measurements. (Elements with atomic numbers higher than strontium [Sr] were below minimum detectable limits [MDLs] and are omitted from the chart for clarity.)

scattered electron images and elemental spectra of the sample from 1/11/2007 at 1257–1315 PST illustrating some of the key particle features. Assuming that the event samples are representative of the material that caused the elevated PM$_{10}$ concentrations, the SEM-EDS data confirms the dominance of geological material.

The Effective Variance (EV)-Chemical Mass Balance (CMB) receptor model (Watson et al., 1984; 2008) was applied to attribute the elevated PM$_{10}$ concentration to pollution sources using local geological source profiles. Potential fugitive dust contributors included: 1) natural soil, 2) paved road dust, 3) cinderblock facility storage pile, and/or 4) concrete facility sand. Absence of an increase in PM$_{2.5}$ mass, and the large increase in PM$_{10}$ crustal-related elements during the event, indicate that sources such as motor vehicle exhaust, residential wood combustion, and secondary sulfates and nitrates could be eliminated as causes of the event. Since Al, Si, and K are not quantifiable owing to the variable blank levels, Ca, Fe, rubidium (Rb), strontium (Sr), yttrium (Y), zirconium (Zr), and molybdenum (Mo) were used as the fitting species in the EV-CMB solution.

For the five PM$_{10}$ event and transition period samples, the best agreement (i.e., R^2 ≥0.96, chi-square <5.5) between measured and fitted chemical species was achieved using the paved road dust profile (RS801 in Table 2) from the curb of the entry to the sampling site at Mitchell Road (see Supplemental Table S-3). Similar contributions but slightly lower performance measures were found for the natural
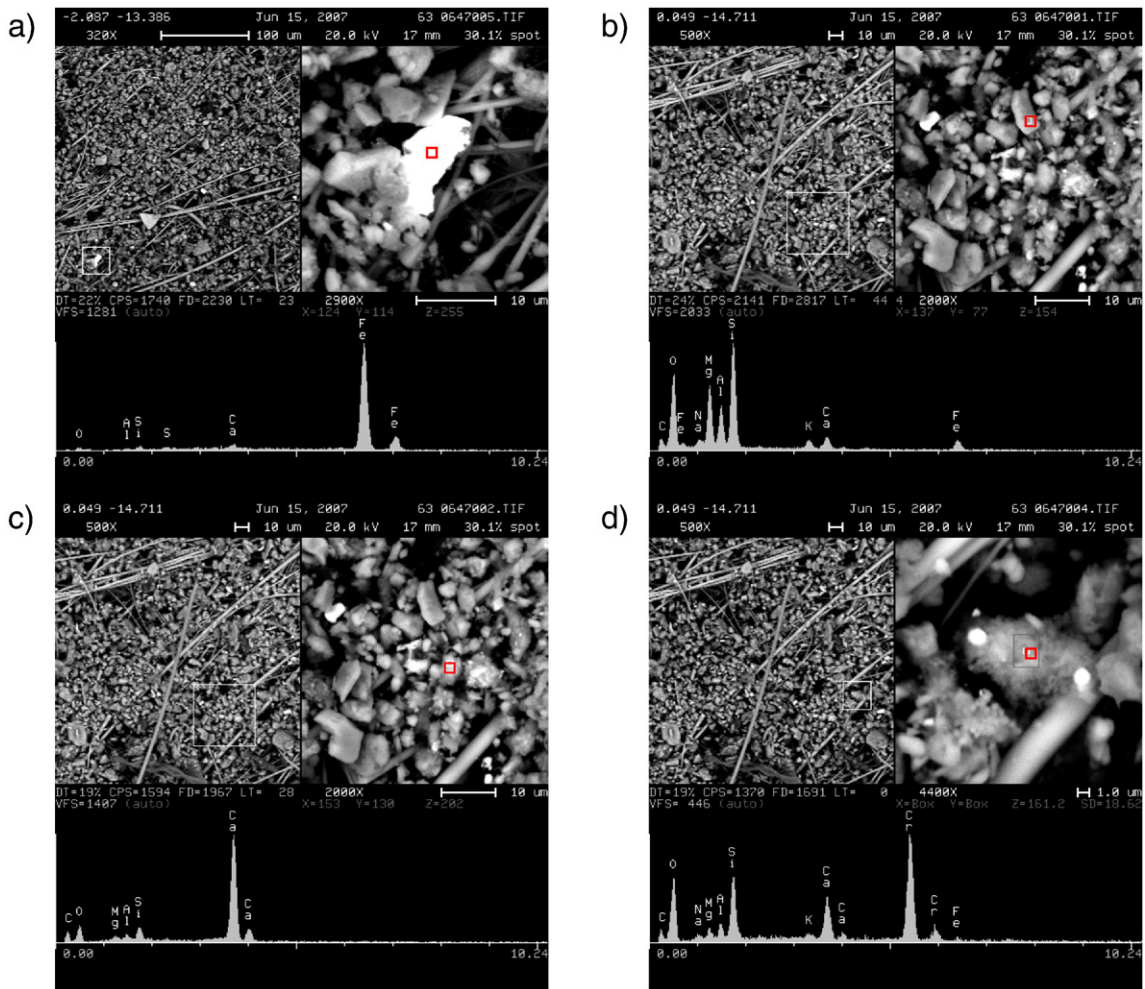
Fig. 5. Backscattered electron images and elemental spectra of the event sample collected at 1257 PST on 1/11/2007 for: a) iron-rich particles; b) silicon/aluminum-rich particles; c) calcium-rich particles; and d) chromium-rich particles. (The top left panel in all four figures shows 500x magnification; the top right panel shows 2000x magnification for Fig. 5a and b and 4400x magnification for Fig. 5c and d; X-ray elemental spectra (at red box) is shown at the bottom of each figure.)

soil, which is consistent with much of the road dust originating from trackout or windblown dust from nearby unpaved areas. Among non-fitting species, S and Cl concentrations report good calculated-to-measured ratios, further supporting paved road dust as the major contributor to this PM_{10} event. Fig. 6 shows the similarity between an event sample (1257–1315 PST on 1/11/2007) and the paved road dust profile (RS801) fitting result, especially for elemental S, Cl, Fe, and Sr. The event sample contains more "non-geological" elements such as nickel (Ni), Cu, cadmium (Cd), tin (Sn), and antimony (Sb) that may result from other sources. Although the cinderblock pile source profile (RS806) reasonably fits the sample, it leads to much higher S and Cl concentration than measured BAM values. The resuspended construction soil (RS800) and concrete facility sand (RS805) profiles do not fit the measured event samples.

Of the potential causes identified, the most probable one was a very isolated exposure of short duration (Hypothesis 4), possibly someone throwing a handful of dirt from the
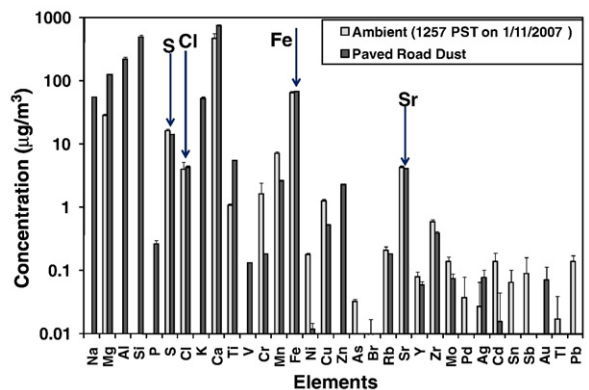

Fig. 6. Comparison between the ambient chemical composition during the event at 1257 PST on 1/11/2007 and CMB fitting with the source profile (i.e., paved road dust; RS801 in Table 2) that shows the best fit with respect to measurable geological elements.

roadway or surrounding soil at the PM_{10} inlet. The fact that there was no corresponding pulse on the nearby $PM_{2.5}$ monitor indicates that only the PM_{10} sampler was affected, and that the dust plume was directed to it. The fact that the tape advanced and that the elemental concentrations increased for the spot as did the mass concentration indicates no instrument malfunction (Hypothesis 1). The lack of high winds along with no corresponding pulse on the $PM_{2.5}$ monitor indicates that the event was not caused by wind erosion (Hypothesis 2). The lack of correspondence between the compositions of material from the nearby industrial sources and the abundances measured on the PM_{10} spot eliminates these sources as contributors (Hypothesis 3).

4. Summary and conclusions

This study illustrates that more information can be obtained from BAM filter deposits to explain high concentrations of short duration. The filter tapes should be time-stamped during site visits and the filters should be changed with gloved hands and stored in refrigerated, sealed containers to preserve them for future analyses. Although blank levels for many elements were high on the BAM glass-fiber filter tape, many of them were consistent, thereby allowing subtraction of background from the deposit values for many useful elements. Aluminum and silicon cannot be quantified as these are the major components of the glass-fiber filter. Even though some material adheres to the back of the tape during its roll-up, the bias is <10%. Analysis of the back side of the filter punches revealed that particles do not penetrate deep into the tape.

Adopting tapes more suitable for elemental analysis should be considered in the development of future BAM systems. The use of glass-fiber filter tape in the BAM limited the type of follow-up chemical analyses. A quartz-fiber filter tape would allow more elements to be retrieved with less interference than glass-fiber. Carbon and ion analyses can also be performed on quartz-fiber filters to achieve mass closure. Since the BAM tape only advances after the attenuation reaches a pre-set loading level or at pre-set time intervals, hourly PM mass concentrations do not correspond to specific event spots. A modification of the BAM sampler software allowing PM concentrations to be directly corresponded to each BAM deposit spot in addition to hourly concentrations is desirable.

Fugitive dust sources have different elemental profiles, especially in industrial areas where raw materials are imported from several locations where the geology differs from that surrounding a sampling site. These PM_{10} source profiles can be used in conjunction with elemental concentrations on the BAM deposits to include or eliminate contributors. These data can be coupled with other measurements, such as wind speeds and directions and corresponding $PM_{2.5}$ measurements to better define the causes of elevated PM_{10} concentrations.

Appendix A. Supplementary data

Supplementary data to this article can be found online at doi:10.1016/j.atmosres.2011.12.004.

References

Casuccio, G.S., Janocko, P.B., Lee, R.J., Kelly, J.F., Dattner, S.L., Mgebroff, J.S., 1983. The Use of Computer Controlled Scanning Electron Microscopy in Environmental Studies. J. Air Pollut. Control Assoc. 33, 937–943.

Chang, C.T., Tsai, C.J., 2003. A Model for the Relative Humidity Effect on the Readings of the PM10 Beta-Gauge Monitor. J. Aerosol Sci. 34, 1685–1697.

Chang, C.T., Tsai, C.J., Lee, C.T., Chang, S.Y., Cheng, M.T., Chein, H.M., 2001. Differences in PM10 Concentrations Measured by Beta-Gauge Monitor and Hi-Vol Sampler. Atmos. Environ. 35, 5741–5748.

Chow, J.C., Watson, J.G., Houck, J.E., Pritchett, L.C., Rogers, C.F., Frazier, C.A., Egami, R.T., Ball, B.M., 1994. A Laboratory Resuspension Chamber to Measure Fugitive Dust Size Distributions and Chemical Compositions. Atmos. Environ. 28, 3463–3481.

Chow, J.C., Watson, J.G., Green, M.C., Lowenthal, D.H., DuBois, D.W., Kohl, S.D., Egami, R.T., Gillies, J.A., Rogers, C.F., Frazier, C.A., Cates, W., 1999. Middle- and Neighborhood-Scale Variations of PM10 Source Contributions in Las Vegas, Nevada. J. Air Waste Manage. Assoc. 49, 641–654.

Chow, J.C., Watson, J.G., Chen, L.-W.A., Arnott, W.P., Moosmüller, H., Fung, K.K., 2004. Equivalence of Elemental Carbon by Thermal/Optical Reflectance and Transmittance With Different Temperature Protocols. Environ. Sci. Technol. 38, 4414–4422.

Chow, J.C., Watson, J.G., Lowenthal, D.H., Chen, L.-W.A., Tropp, R.J., Park, K., Magliano, K.L., 2006. PM2.5 and PM10 Mass Measurements in California's San Joaquin Valley. Aerosol Sci. Technol. 40, 796–810.

Chung, A., Chang, D.P.Y., Kleeman, M.J., Perry, K.D., Cahill, T.A., Dutcher, D., McDougall, E.M., Stroud, K., 2001. Comparison of Real-Time Instruments Used to Monitor Airborne Particulate Matter. J. Air Waste Manage. Assoc. 51, 109–120.

Gehrig, R., Hueglin, C., Schwarzenbach, B., Seitz, T., Buchmann, B., 2005. A New Method to Link PM10 Concentrations From Automatic Monitors to the Manual Gravimetric Reference Method According to EN12341. Atmos. Environ. 39, 2213–2223.

Hauck, H., Berner, A., Gomiscek, B., Stopper, S., Puxbaum, H., Kundi, M., Preining, O., 2004. On the Equivalence of Gravimetric PM Data With TEOM and Beta-Attenuation Measurements. J. Aerosol Sci. 35, 1135–1149.

Huang, C.H., Tai, C.Y., 2008. Relative Humidity Effect on PM2.5 Readings Recorded by Collocated Beta Attenuation Monitors. Environ. Eng. Sci. 25, 1079–1089.

Jaklevic, J.M., Gatti, R.C., Goulding, F.S., Loo, B.W., 1981. A Beta-Gauge Method Applied to Aerosol Samples. Environ. Sci. Technol. 15, 680–686.

Kashuba, R., Scheff, P.A., 2008. Nonlinear Regression Adjustments of Multiple Continuous Monitoring Methods Produce Effective Characterization of Short-Term Fine Particulate Matter. J. Air Waste Manage. Assoc. 58, 812–820.

Lillienfeld, P., 1970. Beta-Absorption-Impactor Aerosol Mass Monitor. AIHA J. 31, 722–729.

Nakamura, M., Ise, H., 1999. PIXE Analysis of Suspended Particulate Matter Originally Collected for Absorption Mass Monitoring. Int. J. PIXE 9, 381–386.

Rodriguez, I., Gali, S., Marcos, C., 2009. Atmospheric Inorganic Aerosol of a Non-Industrial City in the Centre of an Industrial Region of the North of Spain, and Its Possible Influence on the Climate on a Regional Scale. Environ. Geol. 56, 1551–1561.

Saitoh, K., Sera, K., Imaseki, H., Shinohara, M., Fujiwara, M., 2006. PIXE Analysis of Spot Samples of New Type of PTFE Ultra-Membrane Filter Tape Mounted in an Automated Beta-Ray Absorption Mass Monitor. Int. J. PIXE 16, 95–101.

Takahashi, K., Minoura, H., Sakamoto, K., 2008. Examination of Discrepancies Between Beta-Attenuation and Gravimetric Methods for the Monitoring of Particulate Matter. Atmos. Environ. 42, 5232–5240.

Tsai, C.J., Cheng, Y.H., 1996. Comparison of Two Ambient Beta Gauge PM(10) Samplers. J. Air Waste Manage. Assoc. 46, 142–147.

U.S.EPA, 1999. Compendium Method IO-3.3: Determination of Metals in Ambient Particulate Matter Using X-Ray Fluorescence (XRF) Spectroscopy. Report Number EPA/625/R-96/010a. U.S. Environmental Protection

Agency. Center for Environmental Research Information, Office of Research and Development.

Wang, C.F., Chin, C.J., Chiang, P.C., 1998. Multielement Analysis of Suspended Particulates Collected With a Beta-Gauge Monitoring System by ICP Atomic Emission Spectrometry and Mass Spectrometry. Anal. Sci. 14, 763–768.

Watson, J.G., Chow, J.C., 2011. Ambient Aerosol Sampling, In: Kulkarni, P., Baron, P.A., Willeke, K. (Eds.), Aerosol Measurement: Principles, Techniques and Applications, Third Edition. John Wiley & Sons, Inc., Hoboken, NJ, USA, pp. 591–614.

Watson, J.G., Cooper, J.A., Huntzicker, J.J., 1984. The Effective Variance Weighting for Least Squares Calculations Applied to the Mass Balance Receptor Model. Atmos. Environ. 18, 1347–1355.

Watson, J.G., Chow, J.C., Frazier, C.A., 1999. X-Ray Fluorescence Analysis of Ambient Air Samples. In: Landsberger, S., Creatchman, M. (Eds.), Elemental Analysis of Airborne Particles, Vol. 1. Gordon and Breach Science, Amsterdam, pp. 67–96.

Watson, J.G., Chow, J.C., Chen, L.-W.A., Kohl, S.D., 2007. Non-Destructive XRF and SEM Analyses on Beta Attenuation Filters for Elemental Concentrations at the Craig Road Monitor. Desert Research Institute.

Watson, J.G., Chen, L.-W.A., Chow, J.C., Lowenthal, D.H., Doraiswamy, P., 2008. Source Apportionment: Findings From the U.S. Supersite Program. J. Air Waste Manage. Assoc. 58, 265–288.

Zhu, K., Zhang, J.F., Lioy, P.J., 2007. Evaluation and Comparison of Continuous Fine Particulate Matter Monitors for Measurement of Ambient Aerosols. J. Air Waste Manage. Assoc. 57, 1499–1506.